J Solid State Electrochem (2008) 12:1167–1172
DOI 10.1007/s10008-007-0467-1

ORIGINAL PAPER

Characterization and electrochemical study of hemoglobin–carbon nanoparticles–polyvinyl alcohol nanoporous hybrid film

Jing-Jing Yu · Fa-Qiong Zhao · Bai-Zhao Zeng

Received: 8 June 2007 / Revised: 18 October 2007 / Accepted: 22 October 2007 / Published online: 5 December 2007

Abstract A hybrid film is fabricated by casting hemoglobin (Hb)–carbon nanoparticles (CNPs)–polyvinyl alcohol (PVA) suspension on glassy carbon electrode (GCE). The resulting film shows a three-dimensional nanoporous structure. In the hybrid film, the ultraviolet visible (UV–Vis) absorption spectra of Hb keep almost unchanged. The organic–inorganic hybrid material can promote the direct electron transfer of Hb. A pair of well-defined and quasireversible peaks with a formal potential of −0.348 V (vs saturated calomel electrode) is obtained, which is caused by the electrochemical reaction of the Fe(III)/Fe(II) couple of Hb. The electron transfer rate constant (k_s) is estimated to be 3.9 s^{-1}. The immobilized Hb exhibits high stability and excellent electrochemical catalysis to the reduction of oxygen (O_2), hydrogen peroxide (H_2O_2), and nitrite (NO_2^-). The catalytic currents are linear to the concentrations of H_2O_2 and NO_2^- from 1.96 to 112 μM and from 0.2 to 1.8 mM, respectively. Therefore, the hybrid film may be a good matrix for protein immobilization and biosensor fabrication.

Keywords Hemoglobin · Carbon nanoparticles · Polyvinyl alcohol · Nanoporous hybrid film · Direct electrochemistry · Electrochemical catalysis

Introduction

Direct electrochemistry of redox proteins or enzymes has attracted increasing attention in the last decades. It not only can provide information about the electron transfer mechanism of proteins in biological systems, but is also the foundation for fabricating the third-generation biosensors, enzymatic bioreactors, etc. [1, 2]. Hemoglobin (Hb), comprising of four polypeptide subunits (two α and two β subunits) and four hemes, is a typical redox protein. Its physiological function is to store and transport oxygen molecule in the blood of vertebrates [3]. Although Hb does not act biologically or physiologically as an electron carrier, it is an ideal model molecule for the study of electron transfer due to its commercial availability and known structure. However, because its redox centers are usually embedded in the molecules, it is difficult for the electron transfer between Hb and electrode to occur. To realize the direct electrochemistry of Hb, the electrode is generally modified with various functional materials. Up to now, many materials have been used to immobilize Hb on the surface of electrodes to achieve the direct electron transfer, such as surfactants [4], polymers [5–7], nanomaterials [8–12], inorganic mesoporous materials [13–15], and so on. Among them, nanomaterials are widely adopted due to their good biocompatibility and large active surface area, which could provide a desirable microenvironment and facilitate the direct electron transfer of Hb [8–12].

The organic–inorganic hybrid materials, consisting of organic polymer and inorganic nanomaterials, are new matrixes suited for the immobilization of proteins. They possess high biocompatibility and rigidity [16–18]. Different organic–inorganic hybrid materials have been used to immobilize redox proteins on the electrode surface to study direct electrochemistry of the proteins [18, 19]. For example, Zong et al. developed a hybrid material composed of zirconia and grafted collagen for the immobilization of horseradish peroxidase (HRP) [18]. It was found that the hybrid material could promote the electron

J.-J. Yu · F.-Q. Zhao · B.-Z. Zeng (✉)
Department of Chemistry, Wuhan University,
Wuhan 430072, People's Republic of China
e-mail: bzzeng@whu.edu.cn

transfer of HRP. Significantly, the protein electrode showed high thermal and mechanical stability. Jia et al. have used a sol–gel-derived tin oxide/gelatin composite film to immobilize HRP and achieved its direct electrochemistry [19]. The immobilized protein displayed good stability and electrocatalytic activity, too. In this work, we develop a novel hybrid material, which is composed of carbon nanoparticles (CNPs) and polyvinyl alcohol (PVA). Hb is immobilized in it and the resulting modified electrode is studied electrochemically. The Hb–CNPs–PVA film shows three-dimensional nanoporous structure. Hb entrapped in the hybrid material exhibits a pair of well-defined and quasireversible peaks, resulting from its direct electron transfer. The Hb electrode displays high catalytic activity to the reduction of oxygen (O_2), hydrogen peroxide (H_2O_2), and nitrite (NO_2^-).

Experimental

Reagents

Bovine hemoglobin (Mr 65000) was purchased from Sigma. CNPs (Vulcan XC-72 carbon, Cabot, USA) with specific area of about 254 $m^2\ g^{-1}$ and diameter of 30 nm were used as received. PVA (average degree of polymerization, 1,750±50) came from Sinopharm Chemical Reagent (Shanghai). All other chemicals used were of analytical grade and the solutions were prepared with deionized water.

Electrode preparation

Three-milligram CNPs were dispersed in 1 ml *N*,*N*-dimethylformamide with the aid of ultrasonic agitation, and a homogenous black suspension was obtained. One hundred microliters of the black suspension was mixed with 100 μl 5 mg ml^{-1} Hb aqueous solution and 20 μl 3% PVA aqueous solution. The resulting mixture (noted as Hb–CNPs–PVA) was stored at 4 °C.

Before modification, the bare glassy carbon electrode (GCE) was polished to mirror smooth with 0.05 μm Al_2O_3 slurry, rinsed with water, then ultrasonicated in water and ethanol for several minutes. After that, 3 μl of the Hb–CNPs–PVA suspension was transferred onto the GCE surface, and the solvent was evaporated in air overnight. The modified electrode was noted as Hb–CNPs–PVA/GCE. For comparison, CNPs–PVA/GCE and Hb–PVA/GCE were also prepared using a similar procedure. The resulting electrodes were stored in 0.1 M pH 7.0 phosphate buffer solution (PBS) at 4 °C while not in use.

Methods

All voltammetric experiments were performed on a CHI 660A electrochemical analyzer (Chenhua Instruments, Shanghai, China). The working electrode was a modified GCE. A saturated calomel electrode (SCE) and a Pt wire served as reference electrode and counter electrode, respectively. The working solutions were deoxygenated with a nitrogen gas stream for 30 min before measurement, and blanketed with nitrogen atmosphere during measurement. All electrochemical experiments were performed at room temperature (20±2 °C).

The electrochemical impedance spectroscopy (EIS) was recorded with an EG & G Model 273 electrochemical workstation and EG & G Model 5210 lock-in amplifier (PAR, USA) powered by Echem Software. It was performed in 0.1 M pH 7.0 PBS plus 10 μM methylene blue (MB). The frequency range was from 100 mHz to 100 kHz with an amplitude of 5 mV, and the direct current (*dc*) potential was the average peak potential (vs SCE) of the cathodic and anodic peaks.

Ultraviolet visible (UV–Vis) absorption spectra were recorded with a TU-1901 spectrophotometer (Purkinje General Instrument, Beijing, China). The morphologies of Hb–CNPs–PVA and CNPs–PVA films were obtained using a Quanta 200 scanning electron microscopy (SEM; FEI, Holand). Before recording the SEM images, a drop of sample was transferred onto a glass slide and allowed to dry in air at room temperature.

Results and discussion

Characterization of the hybrid films

Figure 1 shows the SEM images of CNPs–PVA and Hb–CNPs–PVA films. The CNPs–PVA film appears to be compact. CNPs are encapsulated in a mushy PVA film. When Hb is introduced, the resulting Hb–CNPs–PVA film presents a three-dimensional porous structure. The porous structure of the Hb–CNPs–PVA film is beneficial to the mass transfer of electroactive species and the stabilization of the dispersed nanoparticles.

EIS has been widely used to characterize the interface properties of the modified electrode. As the formal potential ($E^{o\prime}$, defined as the average of cathodic and anodic peak potentials) of MB is close to that of Hb; it is used as a redox probe in this study. As shown in Fig. 2, the Nyquist plot for the Hb–PVA/GCE is a large semicircle, indicating that the electron transfer resistance is large and the direct electron transfer of Hb in the PVA film is difficult. However, the Nyquist plot of Hb–CNPs–PVA/GCE shows a relative small semicircle. It indicates that CNPs can decrease the

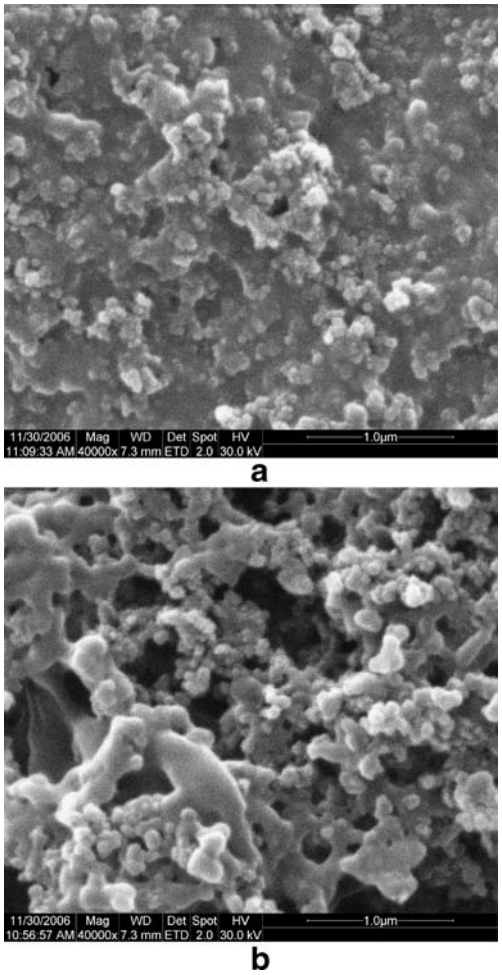

Fig. 1 SEM images of CNPs–PVA (**a**) and Hb–CNPs–PVA (**b**) films on glass slides

electron transfer resistance remarkably, which benefits the direct electron transfer of Hb on the electrode surface.

The position of the Soret absorption bands of heme can provide information about the possible denaturation of the heme protein [20]. Figure 3 shows the UV–Vis spectra of different solutions. The Soret absorption band of the Hb–CNPs–PVA suspension is similar to that of natural Hb, meaning that Hb may still keep bioactivity in the CNPs–PVA suspension. The absorption band shifts 9 nm toward the red in comparison with that of natural Hb (i.e., 405 nm), which can be ascribed to the effect of environment change. The slight shift may be because of the interaction of Hb with CNPs and PVA. It indicates that no denaturation of the immobilized Hb occurs.

Direct electrochemistry of the immobilized Hb

Cyclic voltammograms

Cyclic voltammograms (CVs) of different electrodes in pH 7.0 PBS are displayed in Fig. 4. CNPs–PVA/GCE does not exhibit peaks under this condition, in addition to a large blank current. Hb–PVA/GCE only shows a small irreversible peak. However, Hb–CNPs–PVA/GCE produces a couple of well-defined redox peaks. The peaks should be ascribed to the electrochemical reaction of the heme Fe(II)/Fe(III) couple of Hb. The anodic and cathodic peak potentials are −0.336 and −0.360 V, respectively. The peak-to-peak separation (ΔE_p) is 24 mV, and the cathodic peak current almost equals to the anodic one, indicating that the Hb undergoes a quasi-reversible electrochemical reaction. Therefore, it can be assumed that the CNPs–PVA hybrid film promotes the direct electron transfer of Hb significantly. In this case, the $E^{o\prime}$ is

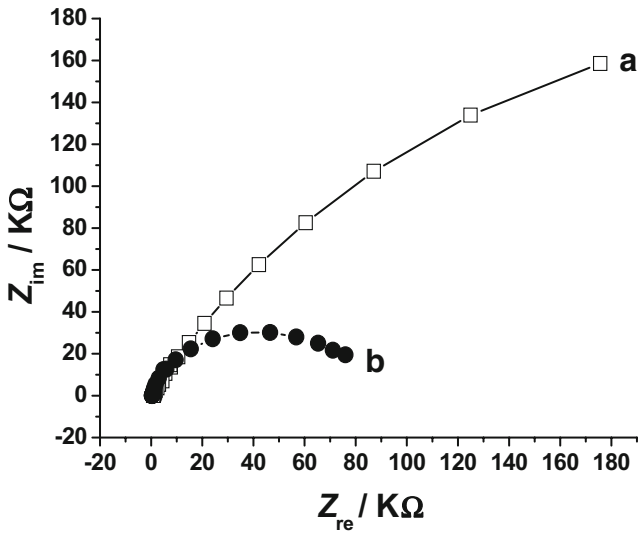

Fig. 2 EIS of different electrodes in 0.1 M pH 7.0 PBS plus 10 μM MB. Electrodes: Hb–PVA/GCE (*a*) and Hb–CNPs–PVA/GCE (*b*); applied potential=−0.254 V

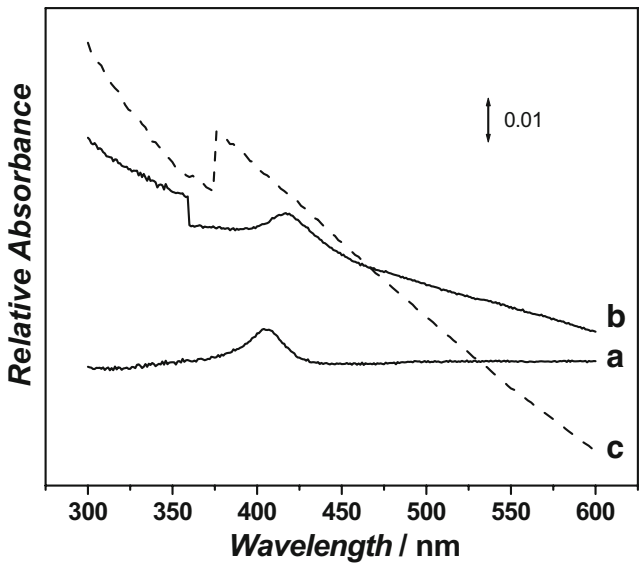

Fig. 3 UV–Vis absorption spectra Hb (*a*), Hb–CNPs–PVA suspension (*b*), and CNPs–PVA suspension (*c*) in pH 7.0 PBS solution

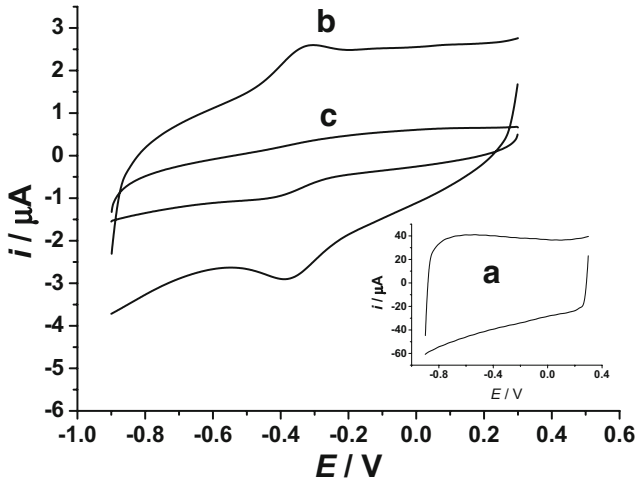

Fig. 4 CVs of different electrodes in pH 7.0 PBS. Electrodes: CNPs–PVA/GCE, (*a*) Hb–CNPs–PVA/GCE (*b*) and Hb–PVA/GCE (*c*); scan rate=0.5 V s^{-1}

−0.348 V, which is close to those reported for Hb immobilized on carbon nanotubes (i.e., −0.342 V) [9] and entrapped in PHEA film (i.e., −0.377 V) [5].

The volume ratio of CNPs to PVA (V_{CNPs}/V_{PVA}) influences CVs significantly. Without PVA, the composite film is unstable. With the decrease of V_{CNPs}/V_{PVA}, the composite film becomes more stable because PVA can form a stable film to immobilize CNPs and Hb on the electrode surface. Meanwhile, the peak currents decrease due to the increase of electron transfer resistance. When the V_{CNPs}/V_{PVA} ratio is 5:1, the composite film is stable enough. Therefore, it is used in this work. Figure 5 presents the EIS of Hb–CNPs–PVA/GCE with different V_{CNPs}/V_{PVA} ratios. They all show a big semicircle and the diameter increases with the decrease of V_{CNPs}/V_{PVA} ratio, indicating that PVA causes big electron transfer resistance.

Effect of scan rate

Figure 6 presents the influence of scan rate (υ) on the CVs of Hb–CNPs–PVA/GCE. With the scan rate increasing from 0.03 to10 V s^{-1}, both the anodic (i_{pa}) and cathodic (i_{pc}) peak currents increase linearly, which reflects the characteristic of a surface-controlled system [14]. Meantime, the ΔE_p changes slightly, but it is smaller than 200 mV, meaning that the electron transfer is faster. When $n\Delta E_p$<200 mV, the electron transfer rate constant (k_s) of Hb should obey the following equation [21]: $k_s=mnF\upsilon/RT$ where m is a parameter related to ΔE_p. In this case, the value of k_s is estimated as 3.9 s^{-1}. It is larger than that reported for Hb immobilized on carbon nanotubes (i.e., 1.25±0.25 s^{-1}) [9], but is much smaller than that immobilized on single-walled carbon nanotubes (i.e., 20±3 s^{-1}) [8] in which a nonlinear regression analysis of the square-wave voltammograms was adopted.

The surface concentration of electroactive species (Γ^*) can be approximately calculated according to the equation [5]: $Q=nFA\Gamma^*$ where n is the number of electron transferred, F is the Faraday's constant, and A is the effective area of the GCE. The effective surface area was estimated to be 1.94×10^{-3} cm^2 using $K_3Fe(CN)_6$ as a probe, according to the Randles–Sevcik equation [22]. Here, Γ^* was estimated to be 5.18×10^{-10} mol cm^{-2}. Compared with the total amount of Hb immobilized on the surface of the electrode (about 5.95×10^{-8} mol cm^{-2}), it can be determined that there is about 0.87% of the immobilized Hb taking part in the electrochemical reaction. The theoretical monolayer coverage for Hb is 1.8×10^{-11} mol cm^{-2} [5]. Hence, it can be proposed

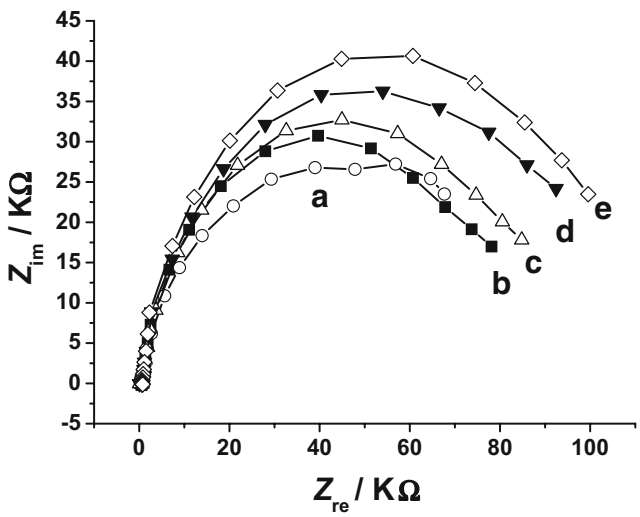

Fig. 5 EIS of Hb–CNPs–PVA/GCE. V_{CNPs}/V_{PVA} ratio=25:1 (*a*), 10:1 (*b*), 5:1 (*c*), 5:2 (*d*), and 5:3 (*e*); other conditions the same as in Fig. 2

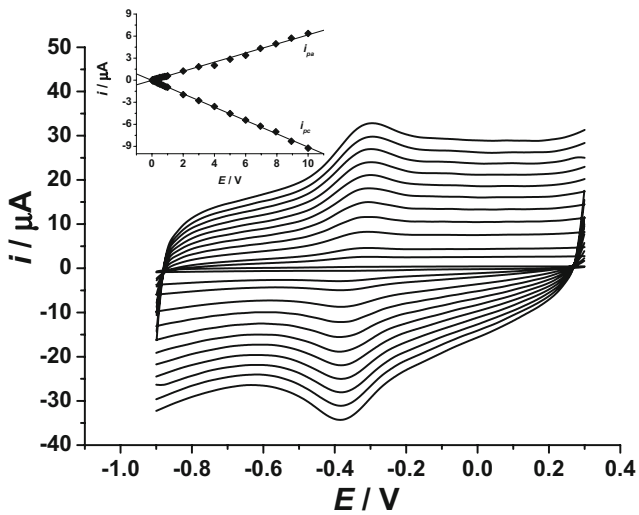

Fig. 6 Effect of scan rate on CVs of Hb–CNPs–PVA/GCE in pH 7.0 PBS. Scan rate=0.05, 0.5, 1, 2, 3, 4, 5, 6, 7, 8, 9, and 10 V s^{-1} (from inner to outer); *inset*, plot of the peak currents vs scan rate

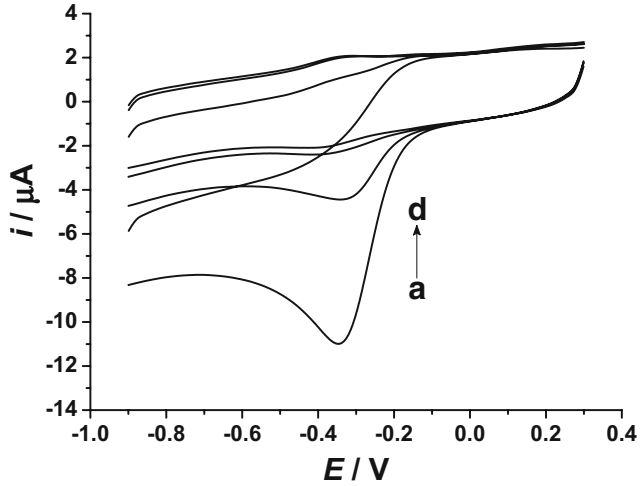

Fig. 7 CVs of Hb–CNPs–PVA/GCE in air-saturated pH 7.0 PBS (*a*) and the solution deoxygenated by nitrogen gas for 1 (*b*), 3 (*c*), and 30 (*d*) min. Scan rate=0.5 V s^{-1}

that several layers of Hb undergo electrochemical reaction, meaning that Hb can exchange electron with the electrode surface through the CNPs–PVA matrix. To test the effect of the CNPs–PVA matrix, a modified electrode with two layers was fabricated through coating a GCE with CNPs–PVA, followed by Hb. As a result, it exhibits a pair of peaks like the Hb–CNPs–PVA/GCE, but the peaks are smaller. This indicates that the three-dimensional porous structure of the hybrid film can transfer electron.

Effect of solution pH

The CVs of Hb–CNPs–PVA/GCE depends on solution pH. When solution pH changes from 3.0 to 10.0, both the anodic and cathodic peak potentials move in negative direction. Moreover, the $E^{o\prime}$ is linear to the pH with a slope of −46.1 mV/pH (R=0.990), which is close to the expected value of −59.0 mV/pH for single proton transfer coupled to single electron transfer [6]. The smaller experimental value should be ascribed to the influence of the protonization of ligands to the heme iron and amino acids around the heme or the protonization of the water molecule coordinated to the central iron ion [6]. In addition, the voltammetric curve is asymmetrical in pH 3.0 solution, but it becomes symmetric again when the modified electrode is put back to pH 7.0 PBS. This results from the reversible conformational change of Hb induced by pH. Therefore, the electrochemical reaction can be simply expressed as follows [23]:

$$\text{Hb Fe(III)} + \text{H}^+ + \text{e}^- \rightarrow \text{Hb Fe(II)} \quad (1)$$

Stability of the Hb–CNPs–PVA hybrid film

The thermal stability of Hb–CNPs–PVA/GCE was investigated. When the temperature increases, the peak currents increases until it is up to 35 °C and then decreases due to the denaturation of Hb. At the same time, the formal potential ($E^{o\prime}$) shifts to the negative direction slightly. However, the Hb–PVA/GCE does not exhibit observable peaks over 35 °C. It indicates that the immobilized Hb has high thermal stability due to the protection effect of the organic–inorganic hybrid nanoporous film.

After 100 successive potential scans, the cathodic peak current of the Hb–CNPs–PVA/GCE decreased by only 2.9%. After the protein electrode was stored in a refrigerator (4 °C) for 10 days, the peak current decreased by 18.3%. Thus, the Hb–CNPs–PVA/GCE is quite stable. Five Hb–CNPs–PVA/

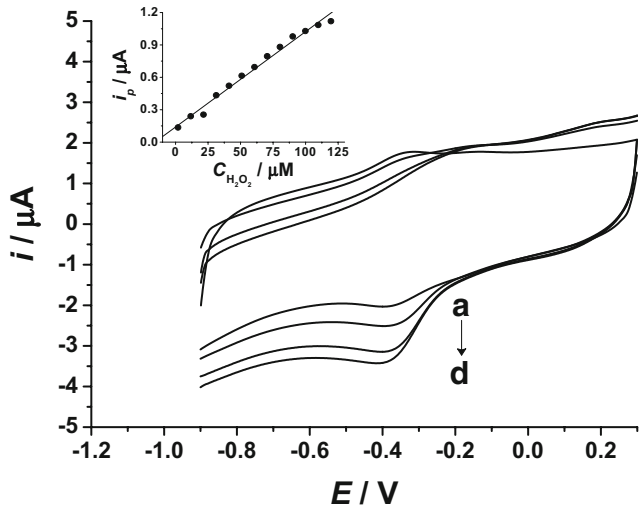

Fig. 8 CVs of Hb–CNPs–PVA/GCE in pH 7.0 PBS containing: 0 (*a*), 41.1 (*b*), 90.1 (*c*) and 119.5 (*d*) μM H_2O_2. *Inset*, plot of the cathodic peak current vs the concentration of H_2O_2; scan rate=0.5 V s^{-1}

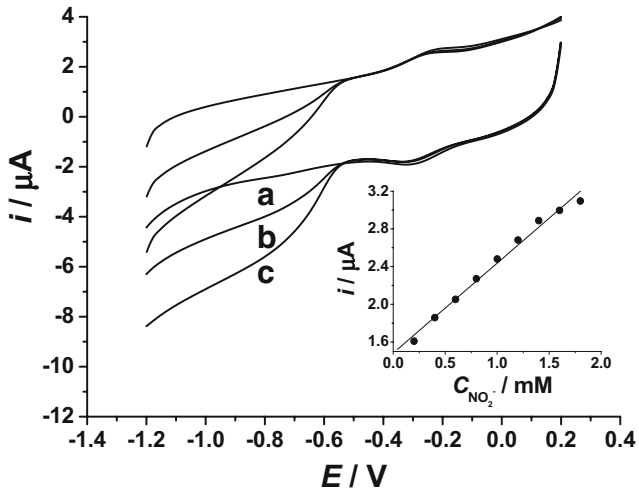

Fig. 9 CVs of Hb–CNPs–PVA/GCE in pH 5.0 PBS containing: 0 (*a*), 1 (*b*) and 3 (*c*) mM NO_2^-. *Inset*, plot of the reduction peak current at 0.8 V vs the concentration of NO_2^-; scan rate=0.5 V s^{-1}

GCEs were fabricated independently; the relative standard deviation (RSD) of the peak current was 7.9%.

Electrocatalytic reduction of O_2, H_2O_2 and NO_2^-

It is well known that heme proteins could catalyze the reduction of many compounds. In this study, the electrocatalytical reduction of O_2, H_2O_2, and NO_2^- on the Hb–CNPs–PVA/GCE has been studied.

Figure 7 shows the CVs of Hb–CNPs–PVA/GCE in the presence of dissolved oxygen. With increasing deoxygenation time, the cathodic peak becomes small. But CNPs–PVA/GCE does not display such behavior. It indicates that Hb–CNPs–PVA/GCE has electrocatalysis to the reduction of O_2. When the experiment is repeated, the catalytic current of O_2 on Hb–CNPs–PVA/GCE almost does not change. This indicates that the redox process of O_2 has almost no influence on the catalytic activity of the immobilized Hb.

With addition of H_2O_2, the cathodic peak of the Hb–CNPs–PVA/GCE increases and the anodic peak decreases (Fig. 8). The cathodic peak current increases linearly with the concentration of H_2O_2 from 1.96 to 112 μM with a correlation coefficient of 0.993. At a higher concentration of H_2O_2, the anodic peak disappears. It indicates that the reduction of H_2O_2 is catalyzed by the immobilized Hb. The electrocatalytic process can be expressed as follows [24]:

$$\text{Hb Fe(III)} + H_2O_2 \rightarrow \text{Compound I} + H_2O \quad (2)$$

$$\text{Compound I} + 2H^+ + 2e \rightarrow \text{Hb Fe(II)} \quad (3)$$

The catalytic current is attributed to the reduction of compound I generated by the reaction of the Hb Fe(III) and it increases with the concentration of H_2O_2 in solution. However, when the concentration exceeds 0.3 mM, the catalytic current even decreases, indicating the inactivation of Hb in the presence of a high concentration of H_2O_2.

As shown in Fig. 9, a new reduction peak at about −0.8 V appears and grows with successive addition of $NaNO_2$. However, under the same condition, the CV of CNPs–PVA/GCE keeps almost unchanged. The cathodic peak current shows linear relationship with the concentration of NO_2^- in the range from 0.2 to 1.8 mM (R=0.994). When the solution pH is higher than 6.0, the reduction peak disappears because it is difficult for the electrochemical reaction to continue [25, 26]. The mechanism can be expressed as follows:

$$3NO_2^- + 2H^+ \rightarrow 2NO + NO_3^- + H_2O \quad (4)$$

$$\text{Hb Fe(II)} + NO \rightarrow \text{Hb Fe(II)} - NO \quad (5)$$

$$\text{Hb Fe(II)} - NO + 2e + 2H^+ \rightarrow \text{Hb Fe(II)} + H_2O + N_2O \quad (6)$$

Conclusions

The hybrid film consisting of Hb, CNPs, and PVA has high stability and shows nanoporous structure. The Hb immobilized in it exhibits good electroactivity and can give a pair of well-defined and quasireversible peaks. It also displays high catalytic activity to the reduction of O_2, H_2O_2, and NO_2^-. Hence, the CNPs–PVA hybrid film provides a model for the study of direct electron transfer of redox proteins and the development of biosensors.

Acknowledgements The authors appreciate the support from the National Nature Science Foundation of China (Grant No. 20173040).

References

1. Ruzgas T, Csoregi E, Emneus J, Gorton L, Markovarga G (1996) Anal Chim Acta 330:123
2. Armstrong FA, Hill HAO, Walton NJ (1988) Acc Chem Res 21:407
3. Lei C, Wollenberger U, Bistolas N, Guiseppi-Elis A, Scheller FW (2002) Anal Bioanal Chem 372:235
4. He XY, Zhu L (2006) Electrochem Commun 8:615
5. Lu Q, Zhou T, Hu SS (2007) Biosens Bioelectron 22:899
6. Liu HH, Tian ZQ, Lu ZX, Zhang ZL, Zhang M, Pang DW (2004) Biosens Bioelectron 20:294
7. Sun H, Hu NF (2006) J Electroanal Chem 588:207
8. Zhao LY, Liu HY, Hu NF (2006) Anal Bioanal Chem 384:414
9. Cai CX, Chen J (2004) Anal Biochem 325:285
10. He PL, Hu NF, Rusling JF (2004) Langmuir 20:722
11. Salimi A, Sharifi E, Noorbakhsh A, Soltanian S (2006) Electrochem Commun 8:1499
12. Lu Q, Hu SS, Pang DW, He ZK (2005) Chem Commun 20:2584
13. Dai ZH, Liu SQ, Ju HX, Chen HY (2004) Biosens Bioelectron 19:861
14. Xian YZ, Xian Y, Zhou LH, Wu FH, Ling Y, Jin LT (2007) Electrochem Commun 9:142
15. Feng JJ, Xu JJ, Chen HY (2006) Electrochem Commun 8:77
16. Giu I, Ballesteros A (1998) J Am Chem Soc 120:8587
17. Cheng X, Dong SJ (2003) Biosens Bioelectron 18:999
18. Zong SZ, Cao Y, Zhou YM, Ju HX (2006) Langmuir 22:8915
19. Jia NQ, Zhou Q, Liu L, Yan MM, Jiang ZY (2005) J Electroanal Chem 580:213
20. George P, Hanania G (1953) Biochem J 55:236
21. Laviron E (1974) J Electroanal Chem 52:355
22. Bard AJ, Faulkner LR (1980) Electrochemical methods. Fundamentals and Applications, Wiley, New York
23. Trushina E, Oda R, Landers J, Mcmurray C (1997) Electrophoresis 18:1890
24. Zhang Z, Chouchane S, Magliozzo RS, Rusling JF (2002) Anal Chem 74:163
25. Barley MH, Takcuchi KJ, Meyer TJ (1986) J Am Chem Soc 108:5876
26. Younathan JN, Wood KS, Meyer TJ (1992) Inorg Chem 31:3280